Open Access Library Journal
2025, Volume 12, e14097
ISSN Online: 2333-9721
ISSN Print: 2333-9705

Characterization of Aquifers Using Electrical Resistivity and Induced Polarization Surveys in River Sosiani Sub-Catchment, Uasin Gishu County, Kenya

Gilbert Kiptanui*, Mary Makokha, Christopher Shisanya

Department of Geography, Kenyatta University, Nairobi, Kenya
Email: *gilbert.kiptanui46@gmail.com

How to cite this paper: Kiptanui, G., Makokha, M. and Shisanya, C. (2025) Characterization of Aquifers Using Electrical Resistivity and Induced Polarization Surveys in River Sosiani Sub-Catchment, Uasin Gishu County, Kenya. *Open Access Library Journal*, **12**: e14097.
https://doi.org/10.4236/oalib.1114097

Received: August 8, 2025
Accepted: September 21, 2025
Published: September 24, 2025

Abstract

Freshwater is a critical resource for domestic and agricultural use, but its occurrence presents a challenge. Utilization of electrical resistivity methods in aquifer delineation underscores their importance in the field of hydrogeology. The Sosiani sub-catchment is a geologically complex area where saline groundwater has been sporadically encountered, and while the electrical resistivity method has been used for groundwater prospecting in the area, it has not been effective in distinguishing between saline and freshwater zones on its own. This research characterized aquifers of Sosiani sub-catchment in terms of salinity using the Electrical Resistivity and Induced Polarization methods that involved 31 Vertical Electrical Soundings. Validation of observed aquifer salinity from ER/IP surveys was performed using Electrical Conductivity tests of 20 water samples collected from boreholes in the sub-catchment. The VES results indicate a shallow saline aquifer at 14 - 37 m and a deep freshwater aquifer at 100 - 193 m. Observations from interpolated aquifer depths indicate a shallow aquifer at 3.7 - 30.2 m and a deep aquifer at 43.0 - 149 m depths. The borehole completion reports from selected boreholes in the sub-catchment also confirm these indicating aquifers at 2 - 35 m, 50 - 85 m and 100 - 195 m depths. An aquifer depth contour map generated in QGIS revealed both aquifers occurring throughout the sub-catchment, with low chargeability and high salinity zones coinciding. The findings of this research indicate that characterization of shallow aquifers in terms of salinity is possible through ER/IP methods. It also provides knowledge on the aquifer distribution and Salinity variation in the Sosiani sub-catchment, which serves as a guide in the siting of groundwater boreholes.

Subject Areas

Hydrology, Geophysics

Keywords

Aquifer, Aquifer Characterization, Induced Polarization, Electrical Resistivity, Sosiani Sub-Catchment, Salinity

1. Introduction

Water is an essential component of life, and its importance is demonstrated by its abundance in proportion when compared to the other components on earth's surface. While most of this resource is available and accessible in oceans, lakes, rivers, glaciers and groundwater aquifers, only 2.5% of it is fresh and therefore useful for the sustenance of life [1]-[3]. 1.2% of the freshwater resources are available, but their access is dictated by nature [4].

Salinity is one of the parameters that is used in the lab to characterize water, and it involves the measurement of the concentration of soluble salts in water expressed as Total Dissolved Solids (TDS) [5]. Electrical Resistivity (ER) and Induced Polarization (IP) field methods have also been applied greatly to characterize groundwater of an area in terms of salinity because of the varying electric responses shown by water at varying levels of salinity [6] [7].

The ER/IP methods have received a wide application including subsurface characterization, groundwater assessment and delineation of fresh and saline zones, saline water intrusion and mapping of groundwater pollution and subsurface geothermal plumes because of their cost-effectiveness in providing valuable subsurface information [6]-[10]. In NW Ireland, for instance, a study on the storage and flow properties of an aquifer using ER done by [8] showed a greater correlation of resistivity data with reference models than when the reference model was based only on borehole observations, indicating their importance in parametrization of groundwater models. Reference [10], while also studying the preferential flow paths of groundwater in Belgium, confirms with [8] that electrical resistivity methods are good at providing hydrogeological model calibration, adding that they also give valuable insights at greater spatial scales. They note, however, that the accuracy of ER methods is limited by the heterogeneity and depths of occurrence of aquifers.

In Africa, ER/IP methods have also been applied and have so far demonstrated tremendous success and reliability. In Algeria, [11] and [12] have done hydrogeological investigations in Chott Ech Chergui Basin and Tebessa municipality, respectively, using these methods, and the aquifer geometries in both studies were clear because of the potentialities portrayed by the resistivity models. Conductive leachates from the nearby landfills in Tebessa further allowed for the monitoring

of the extent of pollution in the aquifers of the Municipality using ER methods. In Tunisia, [13] demonstrated the success of ER/IP methods when they successfully delineated the geometry of Hammam Sayala geothermal plume. From their study, zones of low resistivities and chargeabilities are seen to exhibit a positive correlation with the regions of geothermal upwelling.

Regionally, the electrical resistivity methods have found their application mainly in the field of groundwater potential assessment and have yielded great success, indicated by good-yielding boreholes that have been drilled. From its application in Adilo Catchment in Ethiopia [14], Galgaduud Region in Somalia [15] and Bukombe District in Tanzania [16], the general observation is that electrical resistivity is a reliable method for groundwater assessment.

Electrical Resistivity has also been applied in several regions of Kenya, including Waradey in Wajir [17], among other regions, for groundwater exploration, Kabatini in Nakuru [18] for mapping underground faults, Kanyamwilu in Machakos for ground geophysical mapping [19] and in Naivasha to characterize structural controls of the Olkaria geothermal field [20].

The wide application of the electrical resistivity methods, therefore, in various fields reiterates its importance. It is because of this, therefore, that this research sought to employ ER and IP to delineate the areas and depths of occurrence of the fresh and saline aquifer domains within the Sosiani Sub Catchment area in order to characterize groundwater aquifers to a finer resolution.

2. Materials and Methods

2.1. Study Area

The study area shown by **Figure 1** is located in the Sosiani Sub-catchment area in Uasin Gishu County [21]. The area is bound by the longitudes 35˚6'E and 35˚36'E and latitudes 0˚23'N and 0˚36'N and covers approximately 389.2 km^2.

The regional climate of the area according to [22] is warm and temperate. The area receives a significant amount of rainfall averaging 2027 mm per year with the highest and lowest precipitation received in August and January respectively. The temperatures in the area also average 17.3˚C per year with February being the warmest month at 19.2˚C and July being the coldest month at 15.4˚C.

Vegetation in the Sosiani sub-catchment consists of large fields of forest plantations classified as cultivated terrestrial areas and managed lands under land use land cover classification. There also occur small to medium fields of rain-fed herbaceous crops with sparse trees and shrubs which have been classified as natural and semi-natural terrestrial vegetation [23]. Reference [24] have also noted that tree species including *Makhamia lutea*, *Albizia saman*, *Croton*, *Gravellia robusta*, and *Prunus Africana* occur in the area.

Sosiani Sub Catchment is located in the Uasin Gishu plateau which rises gradually towards the South East and drops gradually towards the North West, with elevations varying between 2079 m and 2329 m above sea level. The plateau is interrupted by occasional hills that were not covered by tertiary phonolitic lava

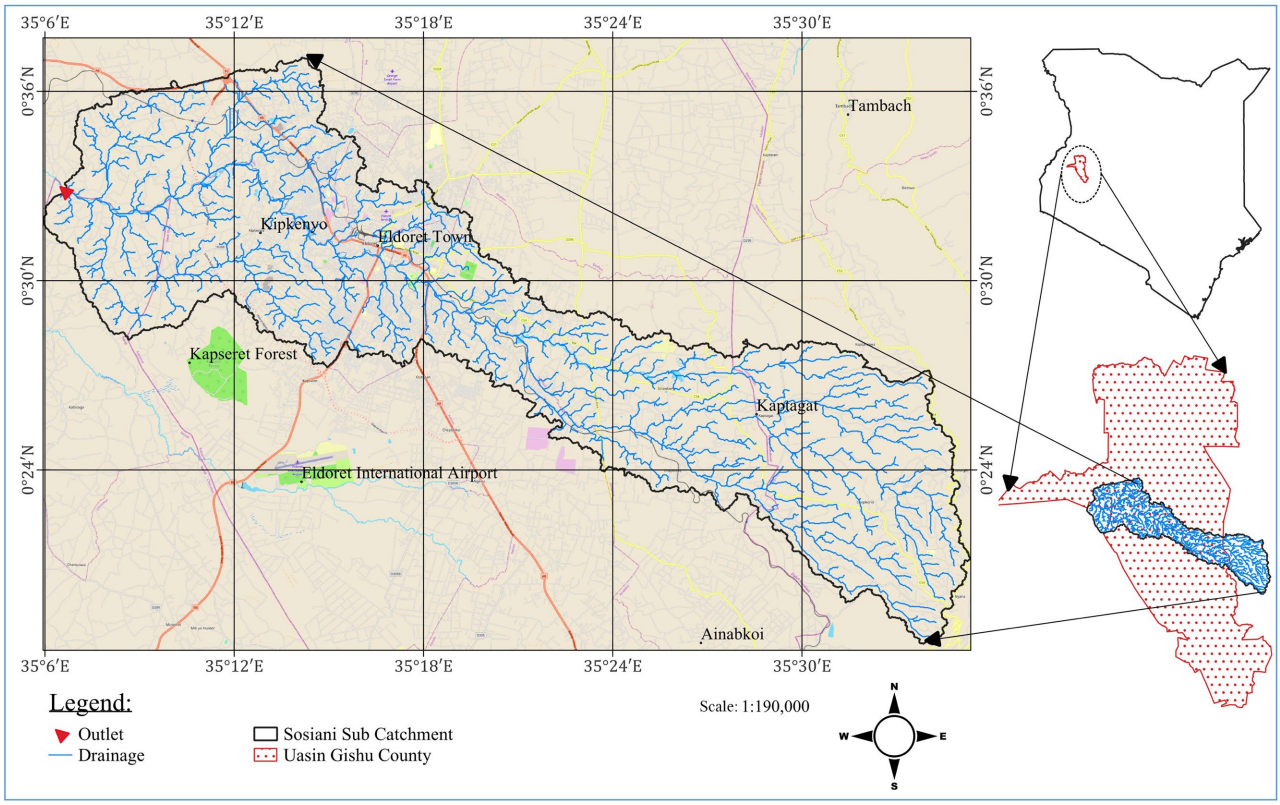

Figure 1. River Sosiani sub-catchment (source: Author).

flows that formed the plateau [25]. The Sosiani sub-catchment is also characterized by several river valleys that give rise to the streams and rivers that drain the catchment towards River Sosiani. River Sosiani drains the catchment into the larger river Nzoia Catchment which further drains into Lake Victoria.

In terms of geology, the Sosiani Sub Catchment area lies within an area that is characterized by Precambrian basement rocks and Tertiary Volcanic rocks of Kenya. The Precambrian basement rocks include the banded microcline Augen-gneisses, metasomatized porphyroclastic sheared gneisses, and mylonites. The volcanic rocks, on the other hand, include the lower and upper Uasin Gishu Phonolites, and Nephelinitic and melanocratic-porphyritic Tindiret Phonolites (**Figure 2**) [25] [26].

According to [27], Sosiani Sub Catchment is characterized by two major soil units. These units include: Orthic Ferralsols covering the largest area (291.8 km^2), and Humic Nitosols covering 97.5 km^2.

According to the Land Use Land Cover Classification, the Sosiani sub-catchment is classified into seven areas [23]. A larger area of the sub-catchment is classified under the cultivated terrestrial areas and managed lands covering approximately 308.1 km^2 followed by the natural and semi-natural terrestrial vegetation classification, covering 59.6 km^2. The rest of the classifications cover small areas, with the Built-up areas classified as artificial surfaces and associated areas covering an approximate 21.5 km^2.

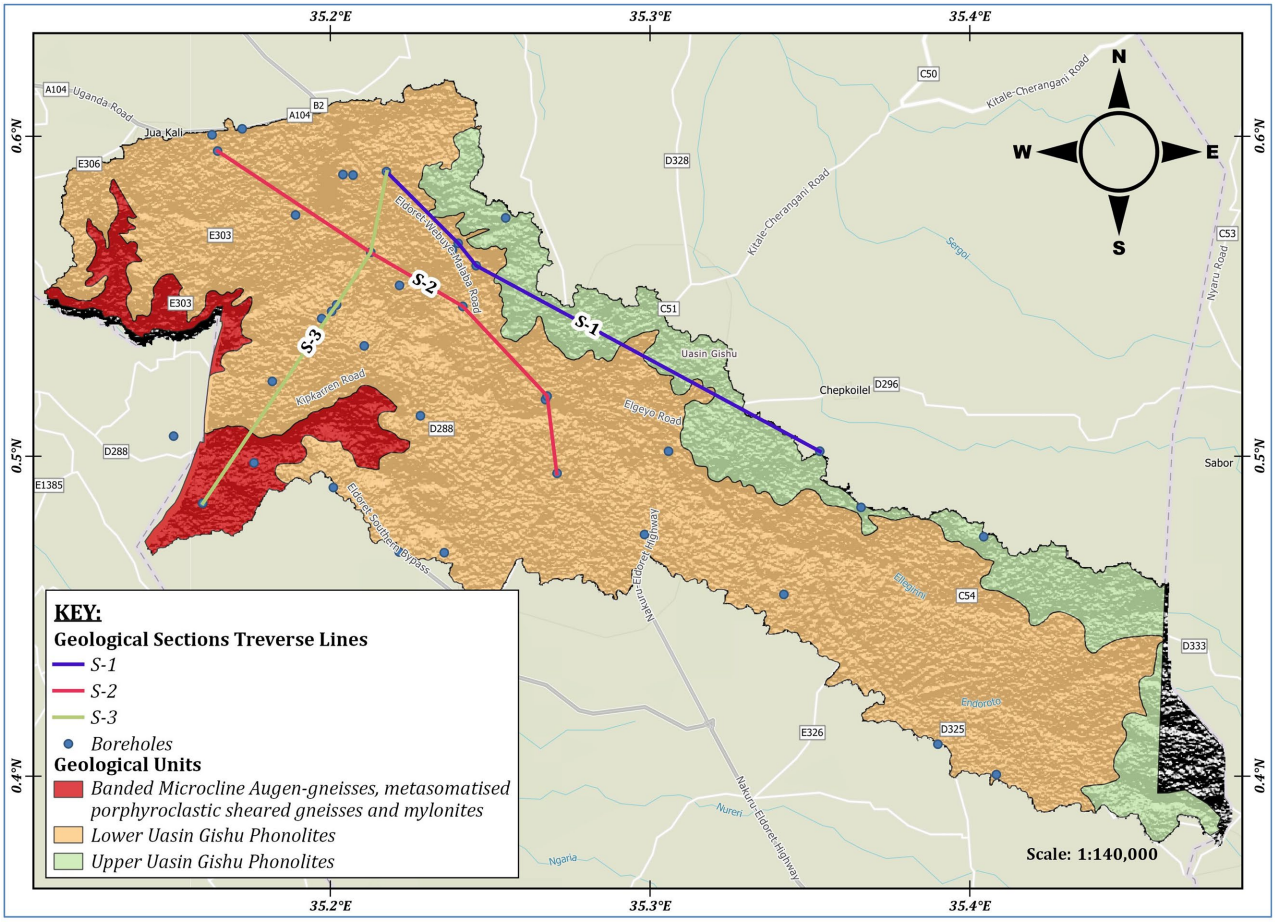

Figure 2. Location of traverse lines of ER/IP Pseudo sections in the Sosiani sub catchment (source: Author).

2.2. Data Sources

Field data collection was undertaken between December 2024 and February 2025. It involved ER/IP surveys and groundwater sampling from identified boreholes. The ER/IP surveys were undertaken using ABEM LS2 resistivity equipment employing the Schlumberger array electrode configuration which has been proven to be reliable in groundwater investigations. In Schlumberger array configuration, the field layout of the electrodes is symmetrical with the spacing between current electrodes (AB) being much greater than the spacing between the potential electrodes (MN). In this configuration, only the current electrodes (AB) are moved progressively increasing the distance between them to an extent where the measured potential difference between the potential electrodes (MN) is too small, necessitating that the potential electrodes be moved also. This layout of electrodes makes the Schlumberger array configuration easier for use in the field compared to other arrays.

EC testing on the other hand was done using Milwaukee MW804 MAX salinity meter after calibration with 20 mL of 12,880 µS/cm Conductivity calibration solution (M10030) before each test.

The appropriate sample size for the ER/IP surveys was determined according

to "Equation (1)" developed by [28].

$$n = N/\left(1 + Ne^2\right) \quad (1)$$

where; n—sample size, N—overall population, and e—Margin of error taken as *0.05*.

A sample size of 38 was calculated from a population of 42 boreholes identified in the sub-catchment. A maximum current electrodes spacing of 400 m was designed for use in ER/IP surveys to achieve a probe depth of 200 m using the Schlumberger array and only 31 boreholes from the calculated sample size met this consideration. The other 7 borehole sites were located in confined spaces where a 400 m maximum spacing of the current electrodes (AB) could not be achieved during a geoelectric VES sounding. However, spatial coverage of the Sosiani sub-catchment and the desired 200 m probe depth was achieved regardless of the encountered field limitations.

Out of the 38 boreholes identified as an appropriate sample size, only 20 boreholes were sampled for Electrical conductivity (EC) testing. The other 18 boreholes were excluded from the sample because of challenges that included: malfunctioned pumps, lack of water in the borehole, and absence of pumps in some of the boreholes. The 20 boreholes sampled for EC testing were however spatially distributed in the Sosiani sub-catchment and therefore provided a reliable representation of the salinity variation in the study area.

Borehole Completion Reports (BCR) for 15 boreholes were obtained from Water Resources Authority Eldoret Regional office and the department of water in Uasin Gishu County. These reports were used to check aquifer depths and geology.

2.3. Data Analysis

2.3.1. Electrical Resistivity

The ER/IP survey data were analyzed in 1D graphs and 2D pseudo sections plotted in IPI2WIN software to understand the variation in resistivity and chargeability in both dimensions. Resistivity and chargeability datasets were manually entered into IPI2WIN software after selecting the Schlumberger array option so that the data analysis matches data collection configurations. The data is then saved and the New Smooth Model option is used in the IPI2WIN software to capture maximum number of layers in the resulting model. An inversion is then run, using the Inversion option, to reduce the data error displayed as Root Mean Square (RMS) error on the title bar of the inferred geoelectric layers table. The RMS is an expression of the difference between the original data and best fit data, so that the higher the RMS the less representative is the produced model and vice versa.

To produce a peudo cross section, several ER/IP interpretation curves of the specific borehole locations are combined using the "add new data" option in IPI2WIN software.

The ER/IP analysis was supported by a validation done through the aquifer trends indicated by the borehole data and the salinity data from the EC tests.

2.3.2. Electrical Resistivity Measurements Uncertainty

To ensure good signal to noise ratio in field measurements, ABEM LS2 terameter was set to utilize current of 500 mA, voltage of 200 V and a power maximum of 200 W. Error propagation into data analysis in IPI2WIN software was also minimized by making sure that the Standard Deviation (Stdev %) for every ER/IP reading during data collection was less than 10%. However, at certain electrode intervals in Emkwen, Naiberi and Ngatit areas, the Stdev % was greater than 10% but it was mitigated by doing repeat measurements.

During 1D data inversion, the RMS error presented in percentage (%) form represented the percentage variance of the observed field data and the produced model. The RMS error varied in the range of 3.73% - 17% giving a confidence level of the resultant models in the range of 83% to 96% (Table 1).

Table 1. Inversion root mean square errors at specific borehole sites.

Borehole Site	RMS Error	Borehole Site	RMS Error
Kingongo	12%	Hill School	10%
S. Kering	12.6%	Lengut	12.8%
Wesley	9.22%	Ngatit	17%
K. Kuku	3.94%	Kapyemit	8.83%
Serem	10.4%	CO Chem	14.9%
Teldet	8.1%	Emkwen	13.6%
Kapsaos	10.8%	Kapserton	3.73%

2.3.3. Electrical Conductivity

The water samples obtained from the field were analyzed for EC in the field using Milwaukee MW804 salinity meter. The EC values obtained were analyzed by plotting its spatial variation in a GIS platform and relating it to the variation in vertical and horizontal resistivities, and chargeabilities in the sub catchment.

2.3.4. Borehole Geology

15 BCR reports containing sub surface geology and water strike data were analyzed in Strater 5 software to present the vertical and lateral variation of the geology and its aquiferous zones in a cross-sectional manner. This analysis was used to validate the aquifer occurrence as indicated by the ER/IP surveys. The mean depth of occurrence of shallow and deep aquifers was also analyzed and presented in a GIS platform to show the spatial variation of each of the aquifers in the area.

3. Results and Discussion

3.1. Spatial Extent and Depth of Occurrence of Saline and Fresh Groundwater Aquifers in Sosiani Sub-Catchment

3.1.1. Electrical Resistivity and Induced Polarization Pseudo Sections

The 2D variation in resistivity and chargeability in the Sosiani sub-catchment was

understood from pseudo sections drawn along traverse lines **S-1**, **S-2** and **S-3** (Figure 2) crossing the different geologic units in the sub-catchment. The pseudo sections (Figure 3) indicate that the apparent resistivity and chargeability in the sub-catchment vary between 25 to 705 Ω·m and 0 to 39 mV/V respectively.

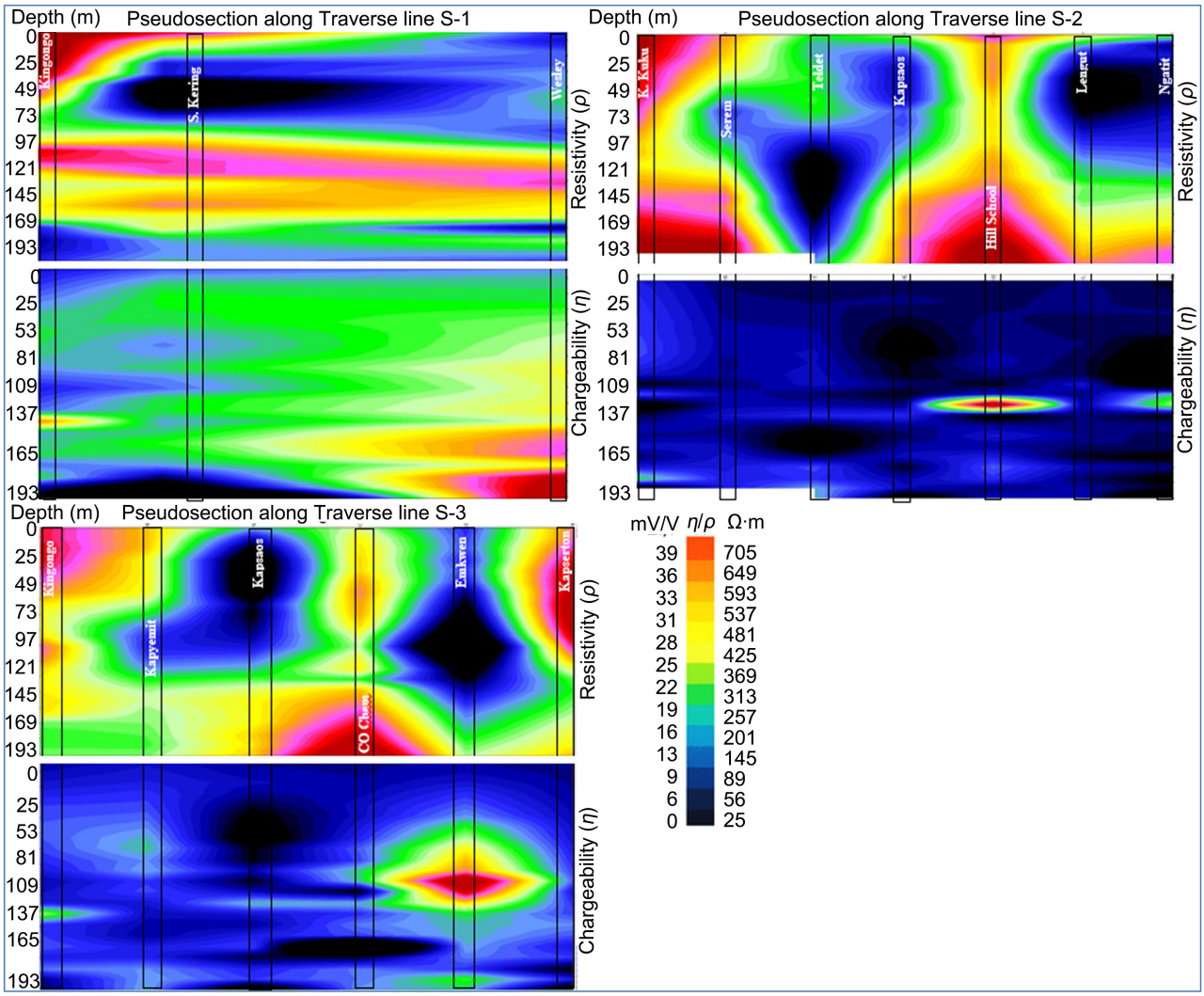

Figure 3. Resistivity and chargeability pseudo sections.

According to the pseudo sections, a shallow aquifer occurs between 14 to 37 m while a deep aquifer occurs between 100 to 193 m, as indicated by the blue to black sections of the resistivity pseudo sections in Figure 3. The aquiferous sections show resistivity lows in the range of 0 Ω·m to 163 Ω·m.

From the ER/IP pseudo sections, the aquifers of the Sosiani sub-catchment are not laterally continuous throughout the sub-catchment. The pseudo section along traverse line **S-1** in Figure 3 presents a shallow aquifer that occurs from the Eldoret municipality and stretches eastwards to Naiberi and Ainabkoi areas. The pseudo sections along traverse lines **S-2** and **S-3** also present isolated aquifers occurring between Kapsaos, Baharini and Emkwen Areas.

The shallow and deep aquiferous zones observed from the ER/IP surveys were interpolated in Quantum GIS using the aquifer depth attribute to show the spatial variation of each of the aquifers in terms of depth in Sosiani sub-catchment as shown in Figure 4. The shallow aquifer in Figure 4(b) is as shallow as 3.7 m on the western parts of the sub-catchment and becomes deeper towards the East extending to 47.9 m. The deep aquifer in Figure 4(a) on the other hand is as shallow as 43 m in the Northern and at the Centre of the sub-catchment and extends to 309 m deep in the North Western part of the sub-catchment.

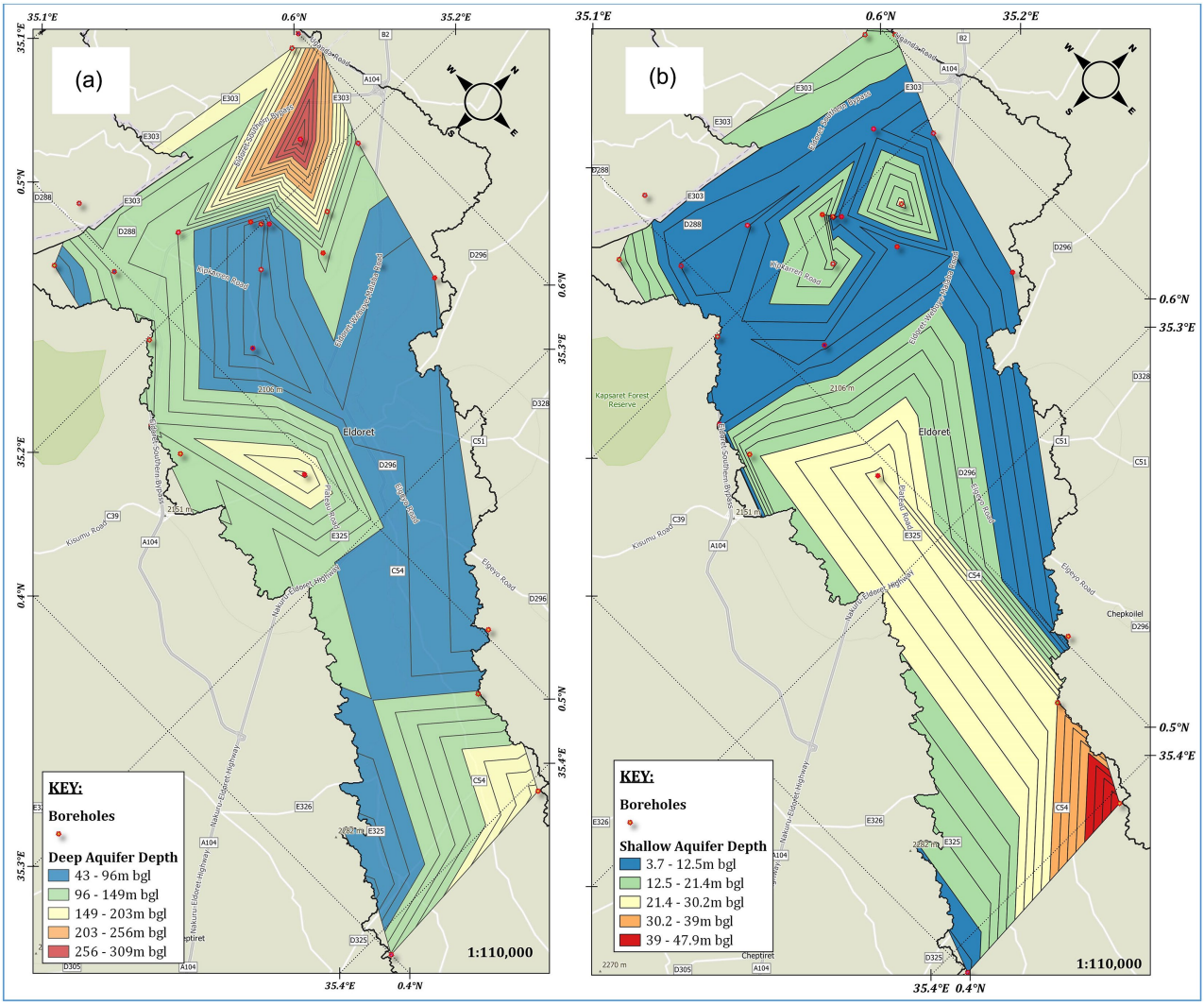

Figure 4. Deep (a) and Shallow (b) aquifers depth variation in sosiani sub catchment (source: Author).

3.1.2. Geological Cross Sections

Geological cross sections drawn from the logs of the already drilled boreholes in the area along the 3 traverse lines **S-1**, **S-2** and **S-3** shown in Figure 2 show the different rock units in the area and the depths at which each of them acts as an aquifer. It is evident from the cross sections that there are three aquifers in the area occurring at 2 to 35 m, 50 to 85 m and 100 - 195 m ranges (Figure 5). The

depth ranges of occurrence of the aquifers according to the geological cross sections are within a similar range for the shallow and deep aquifers observed on the ER/IP pseudo sections, except that an intermediate aquifer occurring between 50 to 85 m is indicated by geological cross sections generated from the BCR. This clearly demonstrates the ability of ER methods in delineating aquifers in a volcanic terrain [20].

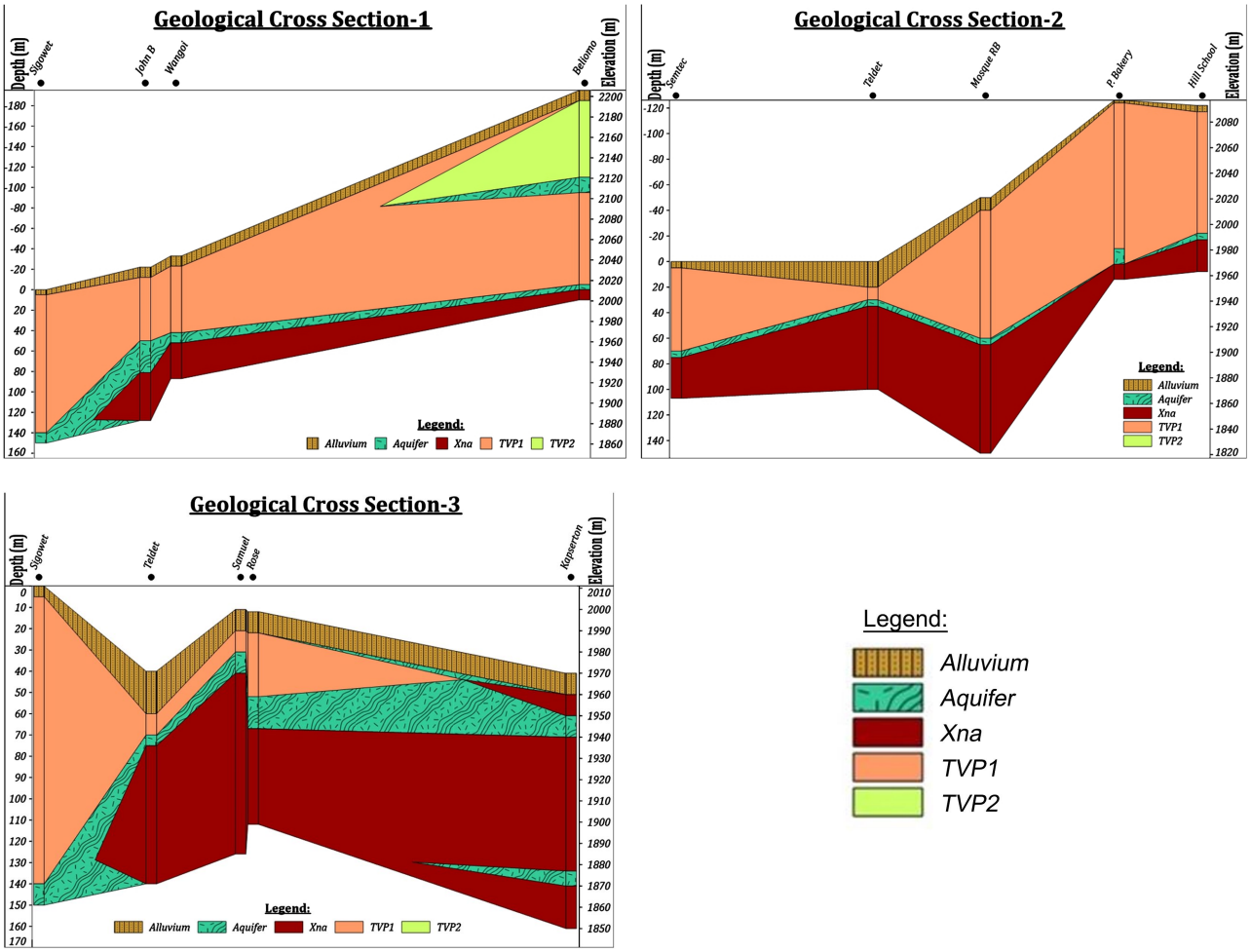

Figure 5. Geological cross sections.

Reference [29] have also been able to map the occurrence of the deeper aquifer to occur at 112 - 130 m depths at the University of Eldoret area, and that aquifer coincides with the 100 - 193 m deep aquifer range in this study. The aquifers mainly occur at the contacts between the different lithological units, concurring with the observation by [30] that some aquifers in Kenya occur at weathered contacts of lava flows. The thickness of a specific lithological unit, therefore, influence the depth of occurrence of an aquifer. The TVP1, TVP2 and Xna geological units, as shown in **Figure 5**, indicate the Lower Uasin Gishu Phonolite, Upper Gishu Phonolite, and the Mylonites and Gneisses rocks, respectively.

The cross sections in **Figure 5** reveal three geological contacts that are aqui-

ferous. The first and shallow contact occur majorly between the alluvium and TVP1 rock and forms an unconfined perched aquifer between Kipkenyo and Lemook Area (**Cross Section - 3**). The pseudo sections in Figure 2 show this alluvial contact extending to 35 m of depth, but appear to vary in depth of occurrence depending on the level of saturation of the alluvium and at the contact. The perched nature of this aquifer between Kipkenyo and Lemook also implies that an impermeable clayey material occurs at the saprolitic zone of weathered TVP1 rock, which inhibits further infiltration of water into the deeper aquifers.

The other geological contacts evident from the geological cross sections include the TVP1 - TVP2 contact and the TVP1-Xna contact. The contact between TVP1 - TVP2 is discontinuous in the Sosiani sub-catchment and only appears to occur around Beliomo area in Illula. The TVP1-Xna contact is deeper and is evidently continuous in the sub-catchment (Figure 5).

3.2. Resistivity and Chargeability of Aquifers at Varying Salinity Ranges

To get the resistivity and chargeability ranges that correspond to groundwater at different salinities in the Sosiani sub-catchment, Electrical Conductivity variation map (Figure 6) was compared with the resistivity and Induced Polarization variation maps at aquifer depths (Figure 7), and aquifers variation maps (Figure 4).

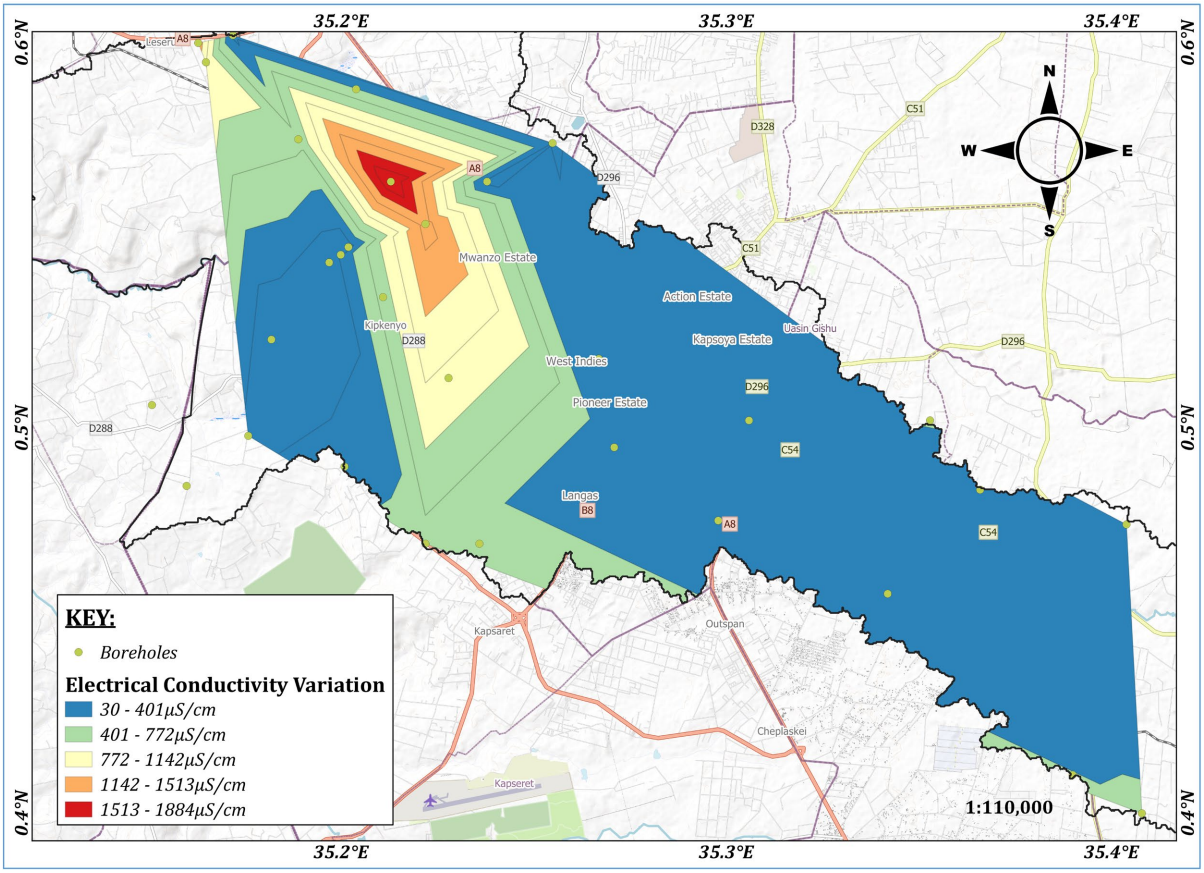

Figure 6. Electrical conductivity variation in the Sosiani sub-catchment (source: Author).

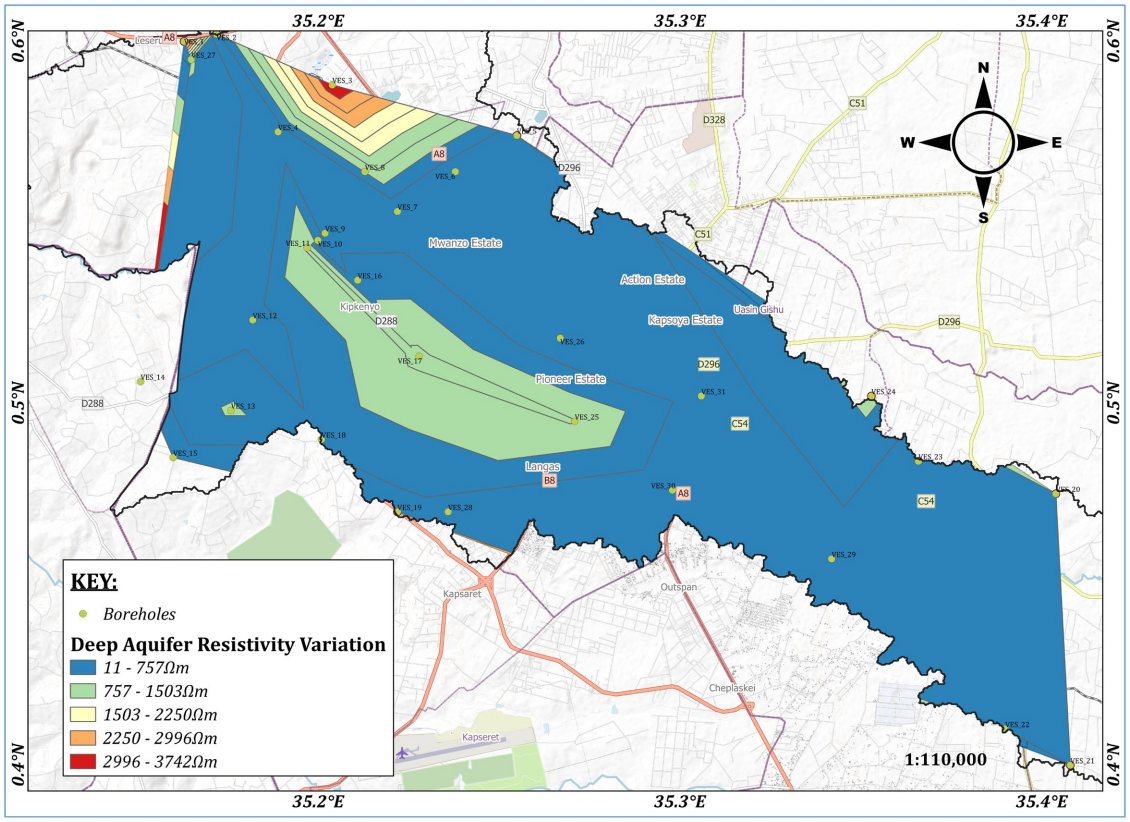
35.2°E
35.3°E
35.4°E
0.6°N
0.5°N
0.4°N
N
S
E
W
Mwanzo Estate
Action Estate
Kapsoya Estate
Pioneer Estate
Langas
Kipkenyo
Uasin Gishu
Kapsaret
Outspan
Cheplaskei
Kapseret
KEY:
Boreholes
Deep Aquifer Resistivity Variation
11 - 757Ωm
757 - 1503Ωm
1503 - 2250Ωm
2250 - 2996Ωm
2996 - 3742Ωm
1:110,000

(a)

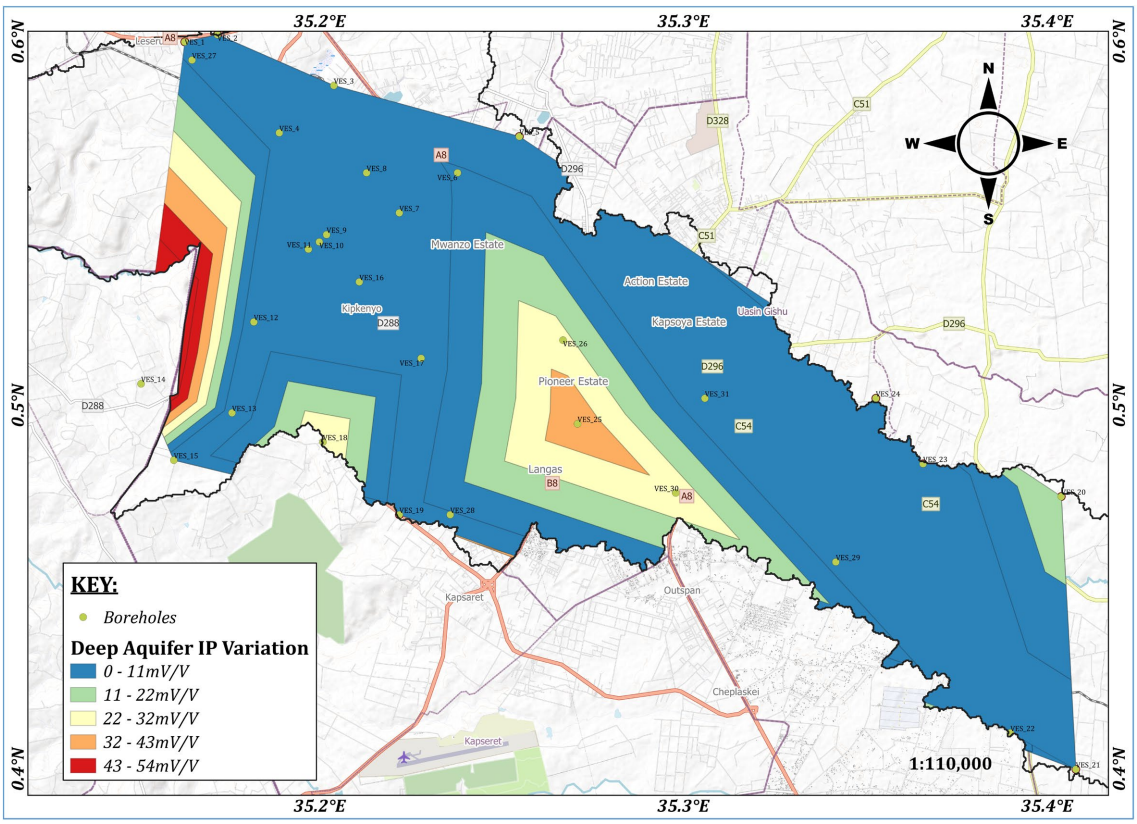
35.2°E
35.3°E
35.4°E
0.6°N
0.5°N
0.4°N
N
S
E
W
Mwanzo Estate
Action Estate
Kapsoya Estate
Pioneer Estate
Langas
Kipkenyo
Uasin Gishu
Kapsaret
Outspan
Cheplaskei
Kapseret
KEY:
Boreholes
Deep Aquifer IP Variation
0 - 11mV/V
11 - 22mV/V
22 - 32mV/V
32 - 43mV/V
43 - 54mV/V
1:110,000

(b)

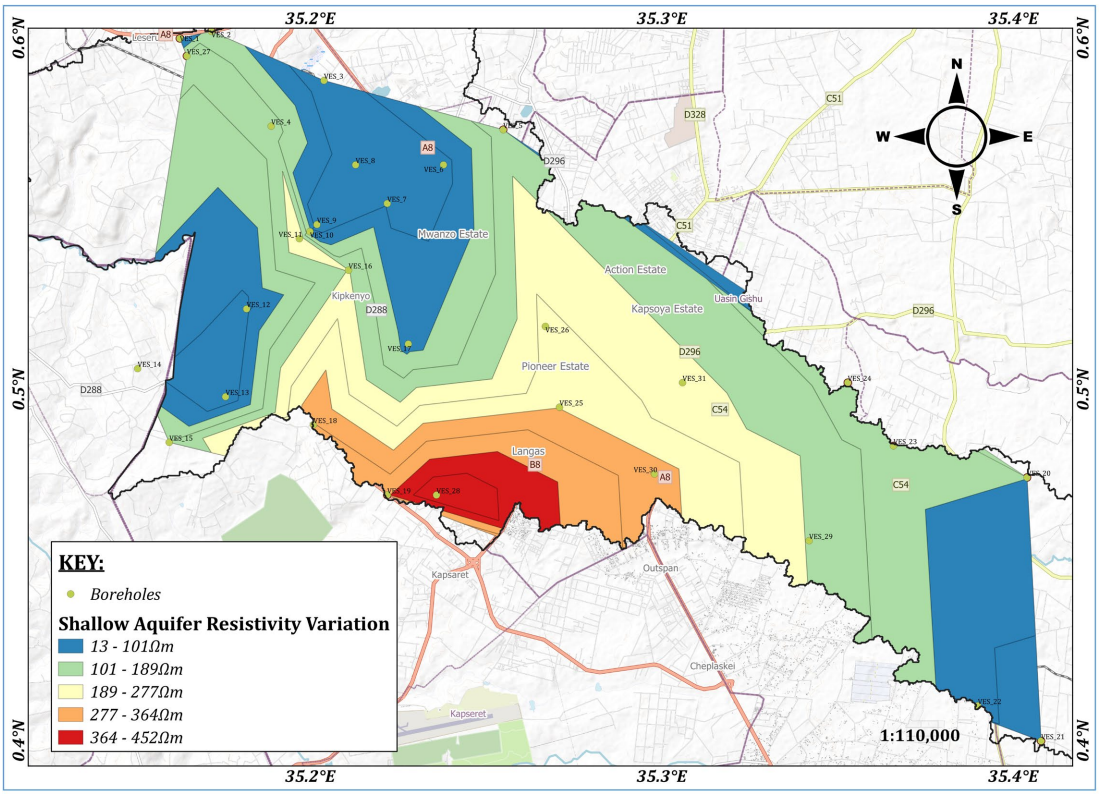

(c)

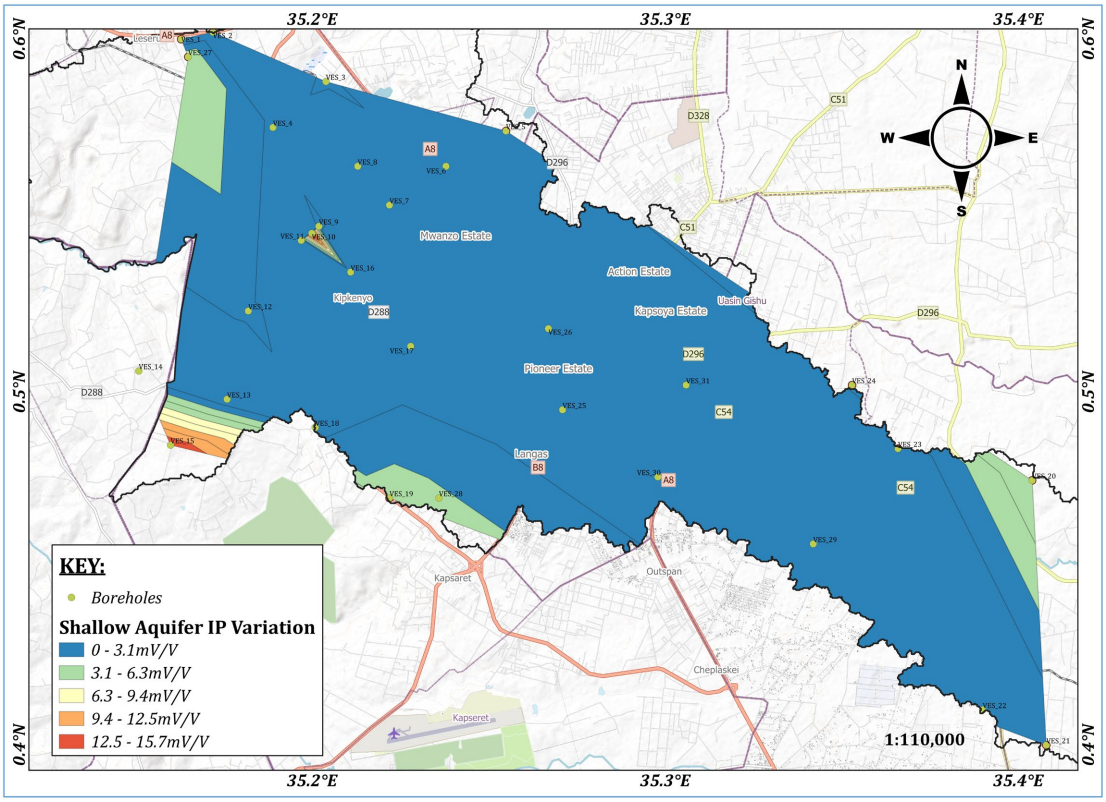

(d)

Figure 7. Aquifers ER and IP Variation in the Sosiani sub catchment (source: Author).

The Electrical Conductivities of the aquifers in Sosiani sub-catchment also majorly vary in the range of 30 - 1142 µS/cm, except for areas around Baharini, Kamagut and Jua kali, recording higher values in the range of 1142 - 1884 µS/cm (**Figure 6**). From the chargeability ranges of both aquifers in **Table 2**, the shallow aquifer is seen to have a lower range of chargeabilities (0 - 3.1 mV/V), suggesting that the higher salinity observed in groundwater is largely contributed by the shallow aquifer. The resistivity variation maps for both shallow and deep aquifers (**Figure 7**) also suggest that the shallow aquifer with a resistivity range of 13 - 277 Ω·m is higher in salinity compared to the deep aquifer with a resistivity range of 11 - 757 Ω·m. This is because higher salinity enhances the electrical conductivity of a material and conversely reduces its electrical resistivity [31].

Table 2. Resistivities and Chargeabilities at different aquifer depths.

Aquifer	Depth (m)			Resistivity (Ω·m)	Chargeability (mV/V)	Salinity (µS/cm)
	Pseudo Section	Variation Map	Geological Cross Section			
Shallow	14 - 37	3.7 - 30.2	2 - 35	13 - 277	0 - 3.1	
Intermediate			50 - 85			30 - 1142
Deep	100 - 193	43 - 149	100 - 195	11 - 757	0 - 11	

The higher salinities/EC, 1142 - 1884 µS/cm, in Baharini, Kamagut and Jua kali areas of this aquifer may also suggest a greater dissolution of salinity-causing ions from the host rocks leading to higher electrical conductivity response (**Figure 6**).

According to the classification of irrigation water by [32] the salinities of water in Sosiani sub-catchment (**Figure 6**) fall into the first three categories: fresh, slightly brackish and brackish with 30 - 600 µS/cm, 600 - 1500 µS/cm and 1500 - 1884 µS/cm salinities respectively as shown in **Table 3** below.

Table 3. Classification of water based on Salinity (adapted from [32]).

Water classification	EC (µS/cm)
Freshwater	<600
Slightly Brackish	600 - 1500
Brackish	1500 - 3000
Medium Saline	3000 - 8000
Saline	8000 - 15,000
Highly Saline	15,000 - 45,000

The resulting chargeability and resistivity lows at the shallow aquifer compared to the deeper aquifer is therefore attributed to the brackish water in the shallow aquifer of the sub-catchment. Higher salinities enhance electrical conduction reducing both resistivity and polarizability of chargeable materials. The deeper aq-

uifer observed to exhibit relatively higher resistivities and chargeabilities imply that its contribution to the general observed salinity of water in the sub-catchment is insignificantly low.

3.2.1. Deep Aquifer

The resistivities of the main deep aquifer at 43 - 149 m bgl depths (**Figure 4(a)**) in the Sosiani sub-catchment majorly range between 11 Ω·m to 757 Ω·m except for higher resistivities at its deeper sections (149 - 309 m bgl) in Kipkenyo, Maili Nne, Kapsaos and Jua Kali areas going to 3742 Ω·m (**Figure 7(a)**). The chargeability of this same aquifer generally varies between 0 - 11 mV/V except for sections of Eldoret town and Lemook areas with chargeabilities going to 54 mV/V (**Figure 7(b)**).

The first level of the deep aquifer at 43 - 149 m bgl predominantly occurs on slightly fractured/weathered lower Uasin Gishu phonolite rock, while the deeper section at 149 - 309 m bgl occurs in weathered mylonites and gneiss basement rocks of higher resistivities [25]. The difference in the resistivity ranges for the two levels of this aquifer is because of the difference in the aquiferous rocks. The 11 - 757 Ω·m aquifer section is hosted in a phonolite rock, which is within the 10 - 10,000 Ω·m resistivity range for volcanic rocks, depending on the grade of weathering and saturation levels of rocks. Based on the borehole geology of the area, the 757 - 3742 Ω·m aquifer section is hosted in basement rocks which have higher resistivities in the range of 1000 - 100,000 Ω·m for unweathered basements and 10 - 1500 Ω·m for their weathered equivalents [33]. These aquifer depths correspond with the stratigraphic layering of the different geologic units of the area (**Figure 5**) confirming their influence on aquifer occurrence and the resulting resistivities.

This aquifer also shows a general IP response of 0 - 11 mV/V suggests the presence of highly polarizable clay material in the aquifer, whose chargeability has been influenced by the presence of water. Reference [34] also noted that while quantifying the influence of different clay minerals on chargeability that an increase in moisture content in a clayey region causes a decrease in the chargeability of the region regardless of the dominating clay mineral. The chargeabilities on the deeper sections of this aquifer at phonolite-basement contacts extend to 54 mV/V, implying a greater level of weathering into a highly polarizable clayey material in this section. Since an increase in saturation level of an aquifer causes a decrease in chargeability, as noted earlier by [34], it then implies that this level of aquifer with high chargeability has low moisture content and therefore is a low-yielding zone of this aquifer. The clay material occurring at the aquiferous interfaces as indicated by higher chargeabilities would result in low resistivities but that observation was not made in this case, implying also that the clayey sections of these aquifers are thin and therefore suffer layer suppression because of the dominance of the adjacent thicker phonolite and basement rocks [7].

3.2.2. Intermediate Aquifer

This aquifer, at 50 - 85 m (**Figure 5**), is only apparent from the geological cross

sections occurring between the lower and upper Uasin Gishu phonolite flows which exhibit same electric responses under similar weathering conditions. Therefore, this aquifer is not detectable in the ER/IP interpretation because of layer equivalence. The principle of equivalence in ER data interpretation is that a conductive layer occurring between two resistive layers with the same lateral conductance would not be visible on a resistivity curve [35].

The visibility of the shallow and deep aquifers from the ER interpretation is because of the greater contrast in resistivities existing between the quaternary alluvium/Saprolitic zones and the Uasin Gishu Phonolite rocks, and the Uasin Gishu Phonolites and the higher resistivity basement rocks. These two aquifers would be masked by layer suppression, however, their detectability in ER interpretation imply that these zones are thicker and are highly saturated with water.

3.2.3. Shallow Aquifer

This aquifer generally occurs at 3.7 - 30.2 m depths (**Figure 4(b)**) and displays resistivities in the range of 13 - 277 Ω·m except for Kapseret, Langas and Pioneer areas, which show higher resistivities of 277 - 452 Ω·m and extending to 47.9 m depths (**Figure 7(c)**). Except for the Kapserton area and Kaptinga area in Kipkenyo, the shallow aquifer almost entirely exhibits low chargeabilities of 0 - 3.1 mV/V (**Figure 7(d)**) in the Sosiani sub catchment, suggesting the presence of low-capacitance material in this aquifer.

There is a high variability of resistivities in this aquifer section, with the aquifer resistivities varying sporadically in the area. This variability suggests a variation in depths of the contact zones between the quaternary alluvial sediments and the Uasin Gishu phonolites, and the level of weathering and saturation.

It is worth noting also that the lack of direct correlation between the EC and ER/IP datasets for both aquifer levels introduces bias in data since not all the sampled boreholes for EC testing were necessarily the same locations where the geoelectric VES sounding were done. While geoelectric sounding VES results offer insights into the geological and salinity variations through apparent resistivity depictions, the EC results provide ground truthing of the true salinities in the specific boreholes that are not necessarily coincident with the boreholes where VES was done. The introduced bias caused by the non-coincidence of the locations for each of the datasets, however, is mitigated by the fact that both datasets were obtained in spatially distributed point locations in the Sosiani sub-catchment.

4. Conclusion

From this research study, it is evident that the use of ER/IP method is viable and reliable in identifying and characterizing aquifers. This is evidenced by the two main aquifers observed to occur at different depths throughout the Sosiani sub-catchment. A shallow aquifer at 3.7 - 30.2 m, revealed to be the major cause of salinity, shows resistivity and chargeability ranges of 13 - 277 Ω·m and 0 - 3.1 mV/V respectively. Deeper at 100 - 193 m, a fresh aquifer detectable at resistivity range of 11 - 757 Ω·m and chargeability range of 0 - 11 mV/V is also observed to occur.

Acknowledgements

Authors thank the County Government of Uasin Gishu and the Water Resources Authority for providing the borehole completion records, and the institutions and individuals that provided access to their boreholes for sampling and ER/IP surveys.

Conflicts of Interest

The authors declare no conflicts of interest.

References

[1] Vedantu (2023) Uses of Water: Importance, Applications & Examples. Vedantu. https://www.vedantu.com/chemistry/uses-of-water

[2] Liu, J., Yang, H., Gosling, S.N., Kummu, M., Flörke, M., Pfister, S., *et al.* (2017) Water Scarcity Assessments in the Past, Present, and Future. *Earth's Future*, **5**, 545-559. https://doi.org/10.1002/2016ef000518

[3] Yang, D., Yang, Y. and Xia, J. (2021) Hydrological Cycle and Water Resources in a Changing World: A Review. *Geography and Sustainability*, **2**, 115-122. https://doi.org/10.1016/j.geosus.2021.05.003

[4] Kay, D. (2009) Water Management. In: Kitchin, R. and Thrift, N., Eds., *International Encyclopedia of Human Geography*, Elsevier, 207-214. https://doi.org/10.1016/b978-008044910-4.00588-5

[5] Clesceri, L.S., Greenberg, A.E. and Eaton, A.D. (1998) Standard Methods for the Examination of Water and Wastewater. American Public Health Association (APHA); American Water Works Association (AWWA); Water Environment Federation (WEF).

[6] Ammar, A.I., Gomaa, M. and Kamal, K.A. (2021) Applying of SP, DC-Resistivity, DC-TDIP and TDEM Soundings in High Saline Coastal Aquifer. *Heliyon*, **7**, e07617. https://doi.org/10.1016/j.heliyon.2021.e07617

[7] Aizebeokhai, A.P. (2014) Assessment of Soil Salinity Using Electrical Resistivity Imaging and Induced Polarization Methods. *African Journal of Agricultural Research*, **9**, 3369-3378.

[8] Comte, J., Ofterdinger, U., Legchenko, A., Caulfield, J., Cassidy, R. and Mézquita González, J.A. (2018) Catchment-Scale Heterogeneity of Flow and Storage Properties in a Weathered/Fractured Hard Rock Aquifer from Resistivity and Magnetic Resonance Surveys: Implications for Groundwater Flow Paths and the Distribution of Residence Times. *Geological Society, London, Special Publications*, **479**, 35-58. https://doi.org/10.1144/sp479.11

[9] Mahmud, S., Hamza, S., Irfan, M., Huda, S.N., Burke, F. and Qadir, A. (2022) Investigation of Groundwater Resources Using Electrical Resistivity Sounding and Dar Zarrouk Parameters for Uthal Balochistan, Pakistan. *Groundwater for Sustainable Development*, **17**, Article ID: 100738. https://doi.org/10.1016/j.gsd.2022.100738

[10] Robert, T.J. (2012) Geophysical Identification, Characterization, and Monitoring of Preferential Groundwater Flow Paths in Fractured Media. Master's Thesis, ORBi-University of Liege.

[11] Aoudia, M., Issaadi, A., Bersi, M., Maizi, D. and Saibi, H. (2020) Aquifer Characterization Using Vertical Electrical Soundings and Remote Sensing: A Case Study of the

Chott Ech Chergui Basin, Northwest Algeria. *Journal of African Earth Sciences*, **170**, Article ID: 103920. https://doi.org/10.1016/j.jafrearsci.2020.103920

[12] Brahmi, S., Baali, F., Hadji, R., Brahmi, S., Hamad, A., Rahal, O., *et al.* (2021) Assessment of Groundwater and Soil Pollution by Leachate Using Electrical Resistivity and Induced Polarization Imaging Survey, Case of Tebessa Municipal Landfill, NE Algeria. *Arabian Journal of Geosciences*, **14**, Article No. 249. https://doi.org/10.1007/s12517-021-06571-z

[13] Chabaane, A., Redhaounia, B. and Gabtni, H. (2017) Combined Application of Vertical Electrical Sounding and 2D Electrical Resistivity Imaging for Geothermal Groundwater Characterization: Hammam Sayala Hot Spring Case Study (NW Tunisia). *Journal of African Earth Sciences*, **134**, 292-298. https://doi.org/10.1016/j.jafrearsci.2017.07.003

[14] Markos, M., Saka, A., Jule, L.T., Nagaprasad, N. and Ramaswamy, K. (2021) Groundwater Potential Assessment Using Vertical Electrical Sounding and Magnetic Methods: A Case of Adilo Catchment, South Nations, Nationalities and Peoples Regional Government, Ethiopia. *Concepts in Magnetic Resonance Part A*, **2021**, Article ID: 5424865. https://doi.org/10.1155/2021/5424865

[15] Hussein, M.A., Ali, M.Y. and Hussein, H.A. (2023) Groundwater Investigation through Electrical Resistivity Tomography in the Galhareri District, Galgaduud Region, Somalia: Insights into Hydrogeological Properties. *Water*, **15**, Article 3317. https://doi.org/10.3390/w15183317

[16] Kubingwa, J.N., Makoba, E.E. and Mussa, K.R. (2023) Integrated Geospatial and Geophysical Approaches for Mapping Groundwater Potential in the Semi-Arid Bukombe District, Tanzania. *Earth*, **4**, 241-265. https://doi.org/10.3390/earth4020013

[17] Amimo, M.O. and Shune, J.A. (2022) Geo-Electrical Resistivity Assessment of the Groundwater Resources Potential of the Waradey Area, Eldas Sub-County, North Eastern Kenya. *International Journal of Progressive Sciences and Technologies* (*IJPSAT*), **32**, 380-394.

[18] Waswa, A.K. (2019) Application of Electrical Resistivity Method in Mapping Underground River Channels: A Case Study of Kabatini Area in the Kenyan Rift Valley. *Universal Journal of Geoscience*, **7**, 1-14. https://doi.org/10.13189/ujg.2019.070101

[19] Kaloki, B.M. (2020) Geophysical Mapping of Kyamwilu Area, Machakos County, Kenya, Using Electrical Resistivity Technique. *International Journal of Science and Research* (*IJSR*), **9**, 1364-1368.

[20] Omollo, P., Nishijima, J., Fujimitsu, Y. and Sawayama, K. (2022) Resistivity Structural Imaging of the Olkaria Domes Geothermal Field in Kenya Using 2D and 3D MT Data Inversion. *Geothermics*, **103**, Article ID: 102414. https://doi.org/10.1016/j.geothermics.2022.102414

[21] Water Resources Authority (2022) Basin Areas. https://wra.go.ke/basin-areas-2/

[22] Climate-Data (2023) Eldoret Climate. https://en.climate-data.org/africa/kenya/uasin-gishu/eldoret-926351/

[23] Gregorio, A.D. and Muchoki, C. (2002) FAO Map Catalog. Food and Agriculture Organization of the United Nations.

[24] Kutuny, G.K., Njeru, J.R. and Mutuma, E. (2022) Influence of Variation in Bio-Physical Factors on Tree Species Structure and Composition in Kapseret Forest, Uasin Gishu County, Kenya. *Journal of Environmental Sustainability Advancement Research*, **8**, 20-28.

[25] Sanders, L.D. (1963) Geology of the Eldoret Area. Geological Survey of Kenya. Government of Kenya.

[26] Jennings, D.J. (1964) Geology of the Kapsabet-Plateau Area. Geological Survey of Kenya. Government of Kenya.

[27] Van Waveren, E.J. (1995) Soil Map of Kenya. Food and Agriculture Organization of the United Nations, Land and Water Development Division. ISRIC Library.

[28] Yamene, T. (1973) Statistics: An Introductory Analysis. John Weather Hill, Inc.

[29] Chelule, F.K., Nyaberi, D.M. and Kipkorir, L.J. (2024) Evaluation of Groundwater Potential Using Electrical Resistivity Method, in University of Eldoret, Uasin Gishu County, Kenya. *International Journal of Novel Research and Development*, **9**, 489-496.

[30] Olago, D.O. (2018) Constraints and Solutions for Groundwater Development, Supply and Governance in Urban Areas in Kenya. *Hydrogeology Journal*, **27**, 1031-1050. https://doi.org/10.1007/s10040-018-1895-y

[31] Attwa, M., Gemail, K.S. and Eleraki, M. (2016) Use of Salinity and Resistivity Measurements to Study the Coastal Aquifer Salinization in a Semi-Arid Region: A Case Study in Northeast Nile Delta, Egypt. *Environmental Earth Sciences*, **75**, Article No. 784. https://doi.org/10.1007/s12665-016-5585-6

[32] Paranychianakis, N.V. and Chartzoulakis, K.S. (2005) Irrigation of Mediterranean Crops with Saline Water: From Physiology to Management Practices. *Agriculture, Ecosystems & Environment*, **106**, 171-187. https://doi.org/10.1016/j.agee.2004.10.006

[33] Palacky, G.J. (1988) 3. Resistivity Characteristics of Geologic Targets. In: Nabighian, M.N., Ed., *Electromagnetic Methods in Applied Geophysics*, Society of Exploration Geophysicists, 52-129. https://doi.org/10.1190/1.9781560802631.ch3

[34] Sarip, M.K. and Madun, A. (2021) The Influence of Clay Minerals towards Resistivity and Chargeability Value for Groundwater Interpretation. *Recent Trends in Civil Engineering and Built Environment*, **2**, 629-637.

[35] Adetola Sanuade, O., Olayide Amosun, J., David Oyeyemi, K., Adesola Olaojo, A., Sanmi Fagbemigun, T. and Idowu Faloyo, J. (2019) Analysis of Principles of Equivalence and Suppression in Resistivity Sounding Technique. *Journal of Physics: Conference Series*, **1299**, Article ID: 012065. https://doi.org/10.1088/1742-6596/1299/1/012065